Digital Generation of Random Forces for Large-Scale Experiments

M. Shinozuka,*
Modern Analysis, Inc., Ridgewood, N.J.
R. Vaicaitis,† and H. Asada‡
Columbia University, New York, N.Y.

Response cross spectral density is determined for a wing structure represented by a discrete system of masses subject to a stationary gust field. Response cross spectral density due to jack loads to be imposed for fatigue testing in a laboratory is then obtained. By employing an equivalence relation between these cross spectral densities and simulation techniques of multivariate random processes, time histories of jack loads are produced. To illustrate the application of this method, two numerical examples for an idealized wing-gust interaction model are presented.

Nomenclature

A_i = wing surface area at ith location
b_{ij} = elements of triangular torsional moment arm matrix
c_h, c_α = damping coefficients of vertical and torsional motion, respectively
$c(x)$ = chord length
C_L = sectional lift coefficient
$d(x)$ = distance between center of gravity and elastic axis
d_{ij} = elements of matrix $\boldsymbol{d}$
$\boldsymbol{d}$ = inverse moment arm matrix
$e(x)$ = distance between aerodynamic center and elastic axis
g_{ij} = inverse of b_{ij}
E = modulus of elasticity
F_j = generalized random force of jth mode
F_i = actuator force at ith location
G = shear modulus
$h_j(t-\tau)$ = impulse response function of the jth mode
$h(x,t)$ = vertical wing motion
$H_j(\omega)$ = frequency response function of the jth mode
i = index
$\underline{i}$ = $\sqrt{-1}$
I = moment of inertia
I_α = mass moment of inertia per unit span of torsional motion about wing elastic axis
j = index
J = mass moment of inertia about wing elastic axis
k_{ij} = stiffness coefficients
ℓ = distance between discrete mass points
$L(x,t)$ = lift due to gust loading
m_i = discrete mass at ith location
M_j = generalized mass of the jth mode
M_B = bending moment due to gust loading
$\bar{M}$ = bending moment due to the actuator loading
$M(x,t)$ = moment loading due to gust
$p(x,t)$ = external random gust loading (pressure)
q_j = generalized coordinate for the ith mode
$R_p(\tau)$ = autocorrelation funcjtion of gust load $p(t)$
$R_M(x_i,x_j,\tau)$ = cross correlation of bending moment
$\underline{R}$ = triangular matrix which is related to matrix $\boldsymbol{S}$
R_{ij} = elements of matrix $\boldsymbol{R}$
$\boldsymbol{S}$ = cross-spectral density matrix corresponding to wing response due to gust loading
$\bar{\boldsymbol{S}}$ = cross-spectral density matrix corresponding to wing response due to the actuator loading
$S_p(\omega)$ = spectral density of gust loading
$S_M(x_i,x_j,\omega)$ = cross-spectral density of bending moment
$S^{\bar{F}}(y_i,y_j;\omega)$ = cross-spectral density of actuator loading
$S_{w_z}(\omega)$ = vertical gust velocity spectrum
t = time
$T(x,t)$ = twisting moment about wing elastic axis
U_∞ = freestream velocity
w = vertical wing displacement
$w_z(t)$ = vertical gust velocity component
x_i = distance which locates discrete masses
$x_\mu - x_i$ = moment arm at ith location ($\mu = i+1$)
y_i = distance which locates actuator force
$\alpha(x,t\times)$ = torsional motion
α = angle of attack
$\mu,\bar{\mu},\nu,\bar{\nu}$ = indices
ξ = damping ratio
ρ = air density
τ = time
ϕ_j = ith modal shape
ψ_{ij} = random phase angles uniformly distributed between 0 and 2π
ω = frequency
ω_j = modal frequencies
Ω = ω/U_∞, reduced frequency

Received Aug. 29, 1974; revision received Aug. 7, 1975. This work was performed by Modern Analysis, Inc., as subcontractor to Fort Worth Division, General Dynamics under U.S. Air Force Materials Laboratory Contract F33615-73-C-5104, A. W. Davis, Project Engineer. The authors are deeply indebted to M.E. Waddoups and D.J. Wilkins of Fort Worth Division, General Dynamics, for their valuable suggestions on the technical contents of this paper as well as for their support.

Index categories: Aircraft Testing; Aircraft Vibration; Structural Dynamic Analysis.

*President. Also Professor of Civil Engineering, Columbia University. Member AIAA.

†Associate Professor of Civil Engineering. Associate Member AIAA.

‡Research Technician. Presently Research Officer, National Aerospace Laboratory, Tokyo, Japan.

I. Introduction

FATIGUE in flight structures is a problem for which no completely acceptable answers are available yet. Even though various modern design and testing techniques are utilized for construction of flight vehicles, flight structures are not completely free from failures attributable to fatigue. Although the need for a large or full scale laboratory test is now generally recognized, particularly for structural components of advanced composite materials, the choice of loading to be imposed remains relatively uncertain. Previous tests indicate that a load history or sequence in service could produce a considerably different damage rate from that due to a simplified sequence used for laboratory purposes[1-5]. Thus, the main purpose of this paper is to obtain an equivalent load for laboratory testing which would produce the same response as sensed by the structure in actual flight.

In fatigue tests of full or large scale structures subject to random loads, it is necessary to produce as close as possible the same response characteristics as observed in actual flight. The mechanical capability of testing equipment in application to full or large scale structures is limited, however, in that the real time simulation is not quite possible when the rate of loading is high, and that distributed load conditions are difficult to reproduce in experiments; in reality, only a finite number of hydraulic jacks can be utilized to reproduce individual concentrated loads. Therefore, an effort has been made in the present study to generate forcing functions to be applied through the jacks which can reproduce the actual response history within a laboratory model at least at a finite number of cross sections.

We recognize that in establishing a sequence of loads for testing that will reflect what an airplane experiences in an actual flight, it is important to reproduce the variations in rms gust velocity throughout the flight and from flight to flight. In fact, this is being accomplished in some recent studies.[6] The present study, however, focuses on the generation of load histories within individual patches of turbulence which are considered to be stationary in approximation.

To obtain such forcing functions the simulation methods developed for multidimensional and multivariate random processes are utilized[7,8] together with Fast Fourier Transform (FFT) technique. The essential feature of this approach is that a random process can be simulated through a series of cosine functions with weighted amplitudes, arbitrary but evenly spaced frequencies (or wave numbers), and random phase angles uniformly distributed between 0 and 2π. For a multidimensional simulation, spectral density of the random process needs to be specified, while for a multivariate simulation cross spectral density matrix is required.

For the purpose of illustration only, a highly simplified example of a flexible airplane wing penetrating a gust region is considered. The airplane rigid body modes and the nonsteady aerodynamic loads are not included. Furthermore, it is assumed that the gust field is composed of only vertical gust velocity, which is taken to be uniform over the wing surface although a stationary random process in time. The wing structure is idealized as a discrete mass system with random forces due to gust applied at each station (Fig. 1). The bending moment response of this wing is obtained by employing the modal method.

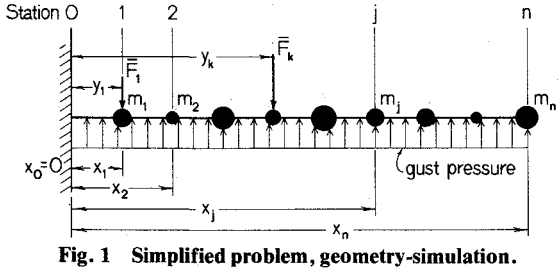

Fig. 1 Simplified problem, geometry-simulation.

II. Structural Analysis

Consider a wing structure represented by a discrete system consisting of n masses as shown in Fig. 1. Disregarding torsional displacements, vertical displacement response at an arbitrary point i can be written as

$$w(x_i,t)=\sum_{j=1}^{M}\phi_j(x_i)q_j(t) \tag{1}$$

in which $\phi_j(x_i)$ is the value of the jth normal mode at $x=x_i$ and $q_j(t)$ the corresponding generalized coordinate. The summation in Eq. (1) extends up to $M(\leq n)$ depending on the necessity. Considering the aerodynamic loading to be quasi-steady and neglecting the aerodynamic forces induced by wing motion due to gust, the equation of motion for the above elastic discrete system can be expressed as

$$\ddot{q}_j+2\xi_j\omega_j\dot{q}_j+\omega_j^2q_j=\frac{1}{M_j}F_j(t) \tag{2}$$

where ξ_j are damping ratios and ω_j natural frequencies. The generalized mass M_j and generalized random force $F_j(t)$ can be written as

$$M_j=\sum_{i=1}^{n}m_i\phi_j^2(x_i) \tag{3}$$

$$F_j(t)=\sum_{i=1}^{n}p(x_i,t)\phi_j(x_i) \tag{4}$$

with $p(x_i,t)$ being the external random gust loading acting on that part of the wing area which is discretized as the ith mass.

By considering that the turbulence field does not change much during the time required for an air particle to pass over the wing, and assuming that it is spatially uniform over the wing surface but varies as a stationary random process, the gust loading spectrum, the response of this wing would be mainly concentrated in the first cantilever bending mode. associated with the ith mass. Then, Eq. (4) reduces to

$$F_j(t)=p(t)\sum_{i=1}^{n}A_i\phi_j(x_i) \tag{5}$$

This kind of gust loading idealization might correspond to a limiting case where a wing span is small in comparison to the scale of turbulence.[9,10] Then for a typical one-dimensional gust loading spectrum, the response of this wing would be mainly concentrated in the first cantilever bending mode.

To find bending moment response at station i, we can write

$$M_B(x_i,t)=\sum_{\mu=i+1}^{n}\sum_{\nu=1}^{n}(x_\mu-x_i)k_{\mu\nu}w(x_\nu,t) \tag{6}$$

in which $x_\mu-x_i$ are moment arms and $k_{\mu\nu}$ stiffness coefficients. Substitution of Eq. (1) into Eq. (6) gives

$$M_B(x_i,t)=\sum_{\mu=i+1}^{n}\sum_{\nu=1}^{n}\sum_{j=1}^{M}(x_\mu-x_i)k_{\mu\nu}\phi_j(x_\nu)q_j(t) \tag{7}$$

By assuming that the random excitation has operated for a sufficiently long time and the effect of initial conditions have died out, response $q_j(t)$ can be written as

$$q_j(t)=\int_{-\infty}^{\infty}h_j(t-\tau)F_j(\tau)\,d\tau \tag{8}$$

where $h_j(t)$ is the impulse response function of the jth mode. From Eqs. (7) and (8)

$$M_B(x_i,t)=\sum_{\mu=i+1}^{n}\sum_{\nu=1}^{n}\sum_{j=1}^{M}(x_\mu-x_i)k_{\mu\nu}\phi_j(x_\nu)\cdot\int_{-\infty}^{\infty}h_j(t-\tau)F_j(\tau)\,d\tau \tag{9}$$

Taking square and then expectation of Eq. (9) and utilizing Eq. (5), the correlation of bending moments at x_i and x_k (autocorrelation if $i=k$ and cross-correlation if $i\neq k$) can be written as

$$R_M(x_i,x_k,\tau)=\sum_{\mu=i+1}^{n}\sum_{\nu=1}^{n}\sum_{j=1}^{M}\sum_{\bar{\nu}=1}^{n}\sum_{\mu'=k+1}^{n}\sum_{\nu'=1}^{n}\sum_{j'=1}^{M}\sum_{\bar{\nu}'=1}^{n}(x_\mu-x_i)\cdot(x_{\mu'}-x_k)A_{\bar{\nu}}k_{\mu\nu}\phi_j(x_\nu)A_{\bar{\nu}'}k_{\mu'\nu'}\phi_{j'}(x_{\nu'})\phi_j(x_{\bar{\nu}})$$

$$\cdot\,\phi_{j'}(x_{\bar{\nu}'})\int_{-\infty}^{\infty}\int_{-\infty}^{\infty}h_j(t-\tau)\,h_{j'}(t+\tau-\tau_1')R_p(\tau_1'-\tau_1)\,d\tau_1 d\tau_1' \tag{10}$$

where $R_p(\tau)$ is the autocorrelation function of $p(t)$ defined in Eq. (5).

Applying the Weiner-Khintchine transform to Eq. (10), the spectral densities (spectral density if $i=k$ and cross spectral density if $i\neq k$) of bending moments are obtained as

$$S_M(x_i,x_k,\omega)=\sum_{\mu=i+1}^{n}\sum_{\nu=1}^{n}\sum_{j=1}^{M}\sum_{\bar{\nu}=1}^{n}\sum_{\mu'=k+1}^{n}\sum_{\nu'=1}^{n}\sum_{j'=1}^{M}\sum_{\bar{\nu}'=1}^{n}(x_\mu-x_i)$$

$$\cdot(x_{\mu'}-x_k)A_{\bar{\nu}}A_{\bar{\nu}'}k_{\mu\nu}k_{\mu'\nu'}\phi_j(x_{\bar{\nu}})\phi_{j'}(x_{\nu'})$$

$$\cdot\phi_j(x_\nu)\phi_{j'}(x_{\bar{\nu}'})H_j(\omega)H_{j'}^*(\omega)S_p(\omega) \tag{11}$$

in which $H_j(\omega)$ is the well known frequency response function of the jth mode, and $S_p(\omega)$ is the pressure spectrum, the Weiner-Khintchine transform of $R_p(\tau)$;

$$H_j(\omega)=(M_j[\omega_j^2-\omega^2+2i\xi_j\omega_j\omega])^{-1} \tag{12}$$

Actuator Loading Corresponding to Bending Moment Spectral Density

To obtain spectral density of the actuator loads for laboratory testing which would produce the same bending moment as described by Eq. (11), consider the wing given in Fig. 1 but with inertia forces neglected. This approximation is valid when the rate of actuator loading is slow, such as in the case of testing full scale wings. Choose a number of points (say r) at stations y (Fig. 1) where the actuator forces $\bar{F}_i$ ($i=1,2,\ldots,r$) are applied on the wing, and obtain a new system of governing equations. The bending moment at some arbitrary point $x_{\bar{\nu}}$ can then be written as

$$\bar{M}(x_{\bar{\nu}},t)=\sum_{\bar{\mu}=\bar{\nu}+1}^{r}(y_{\bar{\mu}}-x_{\bar{\nu}})\bar{F}_{\bar{\mu}}(t) \tag{13}$$

where $\bar{\nu}=0,1,2,\ldots,r-1$. By inverting the above equation, the applied forces $\bar{F}_i$ can be found as

$$\bar{F}_i=\bar{F}(y_i,t)=\sum_{\bar{\nu}=0}^{r-1}d_{i\bar{\nu}}\bar{M}(x_{\bar{\nu}},t) \tag{14}$$

where $i=1,2,\ldots,r$, and the elements $d_{i\bar{\nu}}$ can be found by inverting the moment arm matrix $[\bar{L}]$

$$[d]=[\bar{L}]^{-1} \tag{15}$$

with

$$[\bar{L}]=\begin{bmatrix} y_1-x_0 & y_2-x_0 & \cdots & y_r-x_0 \\ & y_2-x_1 & \cdots & y_r-x_1 \\ & & & \\ 0 & & & \\ & & & y_r-x_{r-1} \end{bmatrix} \tag{16}$$

The fact that Eq. (13) is a square-matrix transformation is significant. It implies that to reproduce the response spectral density at n points on the structure, we need to apply the same number n of actuator loads.

Then, spectral density corresponding to actuator loads $\bar{F}_i$ is

$$S^{\bar{F}}(y_i,y_j,\omega)=\sum_{\bar{\nu}=0}^{r-1}\sum_{\bar{\nu}=0}^{r-1}d_{i\bar{\nu}}d_{j\bar{\nu}}S_{\bar{M}}(x_{\bar{\nu}},x_{\bar{\nu}'},\omega) \tag{17}$$

By setting $S_{\bar{M}}=S_M$ we obtain the required spectral density for the actuator loading. In this way we can take the effect of inertia into account. Thus,

$$S^{\bar{F}}(y_i,y_j,\omega)=\sum_{\bar{\nu}=0}^{r-1}\sum_{\bar{\nu}'=0}^{r-1}d_{i\bar{\nu}}d_{j\bar{\nu}'}S_M(x_{\bar{\nu}},x_{\bar{\nu}'},\omega) \tag{18}$$

where S_M is given in Eq. (11).

Utilizing simulation procedures[7,8] of multivariate random processes (see Appendix), time histories of actuator loading can be produced using the spectral density given in Eq. (18).

To obtain spectral density $S_p(\omega)$ necessary in Eq. (11), consider the beam to be of unit width. Then, the lift force acting on the wing through elastic axis per unit length is

$$L(t)=p(t)=\frac{1}{2}\rho\frac{dC_L}{d\alpha}U_\infty^2\left(\frac{w_z(t)}{U_\infty}\right) \tag{19}$$

in which $dC_L/d\alpha$ = lift curve slope. Taking the lift-curve slope to be a constant along the span and equal to 2π, spectral density corresponding to the lift force is

$$S_p(\omega)=(\pi\rho U_\infty)^2S_{w_z}(\omega) \tag{20}$$

where the vertical gust spectrum $S_{w_z}(\omega)$ is taken to be[12]

$$S_{w_z}(\omega)=6.6976\omega^{-1.4331};\ \text{ft}^2/\text{sec}$$

$$\left.\begin{array}{l}\text{for } \omega\geqq 0.391 \text{ rad/sec, and}\\ \text{for } 0\leqq\omega\leqq 0.391, \text{ rad/sec}\end{array}\right\}=15.9 \tag{21}$$

In Eq. (21), the proper transformation from $S_{w_z}(\Omega)$, $\Omega=\omega/U_\infty$, to $S_{w_z}(\omega)$ for $U_\infty=800$ fps has been included.

III. Numerical Examples

a) Two-mass Discrete System. Consider an airplane wing idealized by a structure shown in Fig. 2. For this structure, mass and influence coefficient matrices are, respectively,

$$[m]=\begin{bmatrix} 6m & 0 \\ 0 & m \end{bmatrix} \tag{22}$$

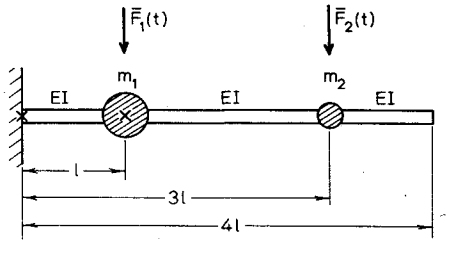

$m_1 = 6m_2 = 6m$

×: locations at which moments are computed

Fig. 2 Two mass system.

$$[a] = \ell^3/6EI \begin{bmatrix} 2 & 8 \\ 8 & 54 \end{bmatrix} \tag{23}$$

Then, the stiffness matrix can be found from

$$[k] = [a]^{-1} = EI/11\ell^3 \begin{bmatrix} 81 & -12 \\ -12 & 3 \end{bmatrix} \tag{24}$$

Natural vibration frequencies can be obtained from

$$| [a][m] - ([I]/\omega^2) | = 0 \tag{25}$$

in which $[I]$ is the identity matrix. Solving Eq. 25

$$\omega_1 = 0.317\left(\frac{EI}{m\ell^3}\right)^{1/2}, \omega_2 = 1.18\left(\frac{EI}{m\ell^3}\right)^{1/2} \tag{26}$$

Corresponding to these frequencies, the normal modes are

$$\{\phi_1\} = \begin{Bmatrix} 0.168 \\ 1.0 \end{Bmatrix}, \quad \{\phi_2\} = \begin{Bmatrix} 1.036 \\ -1.0 \end{Bmatrix} \tag{27}$$

For the purpose of this study, we choose $\ell = 9$ ft, $EI = 3 \times 10^6/144$ lb-ft^2, $m = 1600/32.2$ lb-sec^2/ft, $U_\infty = 800$ fps, and $\rho = 0.0089$ lb-sec^2/ft^4 (30,000 ft altitude). Then, $\omega_1 = 17.5$ rad/sec, $\omega_2 = 64.4$ rad/sec. Taking $A_1 = 1.5\ell$, $A_2 = 2\ell$ and $n = 2$, bending moment spectral density is obtained from Eq. (11) in terms of pressure spectral density $S_p(\omega)$. Numerical values of bending moment spectral density at $x_0 = 0$ and $x_1 = \ell$ are plotted in Fig. 3. The spectral density of actuator forces is shown in Fig. 4. The time histories of the actuator forces are plotted in Figs. 5 and 6.

b) Wing of a Jet Transport. Consider a wing of a jet transport as shown in Fig. 7. The wing is idealized as a discrete mass system shown in Fig. 8. For this wing consider the mass and influence coefficient matrices to be

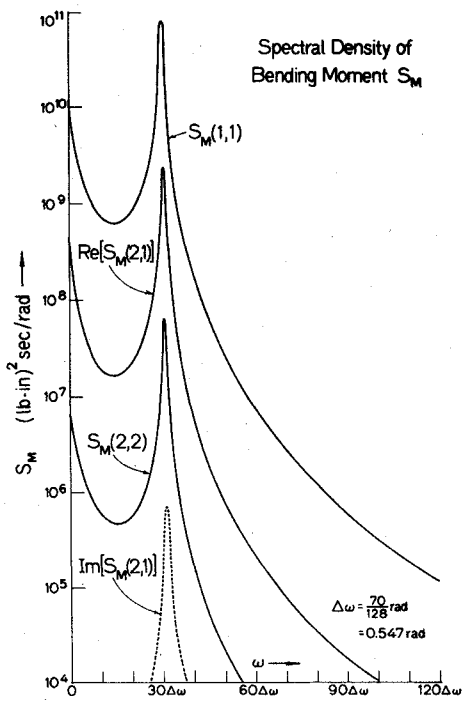

Fig. 3 Spectral density of bending moment S_M.

To obtain the surface areas A's, wing area is divided into five trapezoidal areas. The vector $\{A\}$ is then found to be

$$\{A\} = \begin{Bmatrix} 2.828 \\ 1.391 \\ 1.109 \\ 1.598 \\ 0.525 \end{Bmatrix} \times 10^4 \text{ in}^2 \tag{31}$$

$$[m] = \begin{bmatrix} 6039 & & & & \\ & 10{,}200 & & & \\ & & 4200 & & \\ & & & 3400 & \\ & & & & 680 \end{bmatrix} 1/386 \text{ (lb-sec}^2\text{)/in.} \tag{28}$$

$$[a] = \begin{bmatrix} 72.410 & 144.771 & 150.995 & 195.081 & 231.794 \\ 114.771 & 253.306 & 461.299 & 714.949 & 943.234 \\ 150.995 & 461.299 & 1247.53 & 1911.22 & 2508.54 \\ 195.081 & 714.944 & 2911.22 & 1649.96 & 5237.42 \\ 231.794 & 943.234 & 2508.54 & 5237.54 & 8434.02 \end{bmatrix} \times 10^{-7} \text{ in/lb} \tag{29}$$

Variation of EI with span is assumed to be as shown in Fig. 9.[9] Limiting analysis to the first two bending modes, the first two natural frequencies and normal modes for this structure are determined as

$$\{\phi_1\} = \begin{Bmatrix} 0.084 \\ 0.146 \\ 0.374 \\ 0.591 \\ 1.000 \end{Bmatrix} \quad \{\phi_2\} = \begin{Bmatrix} 0.154 \\ 0.221 \\ 0.272 \\ -0.051 \\ -1.000 \end{Bmatrix} \tag{30}$$

Bending moment spectral density is then obtained from Eq. (11) for $n = 5$ at three locations, i.e. $x_0 = 0$, $x_1 = 90$ in., $x_2 = 186$ in. It is assumed that actuator forces for this case are placed at $y_1 = 186$ in., $y_2 = 368$ in., and $y_3 = 458$ in. The time histories of these loads are plotted in Figs. 10-12.

As can be observed from these results, spectral densities of wing bending exhibit sharp peaks at natural mode frequencies where the wing response is mainly concentrated in the first bending mode. Similar peaks occur in actuator loading spectral densities. If nonsteady aerodynamic loading is included in the formulation, these peaks would be suppressed and response spectral densities would show a wider band random process characteristic. Furthermore, the time histories shown

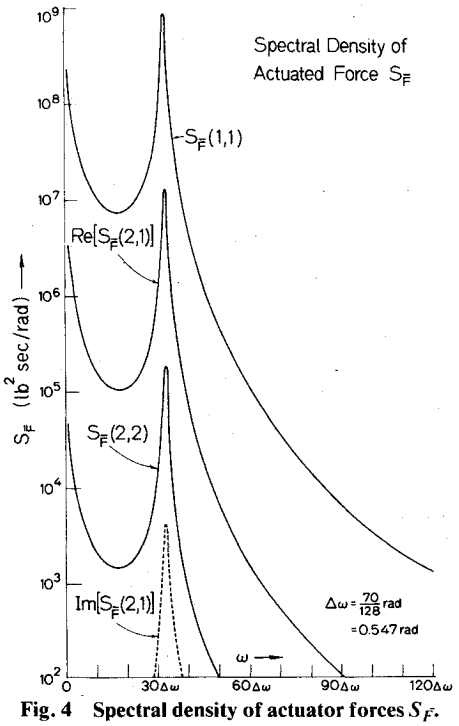

Fig. 4 Spectral density of actuator forces S_F.

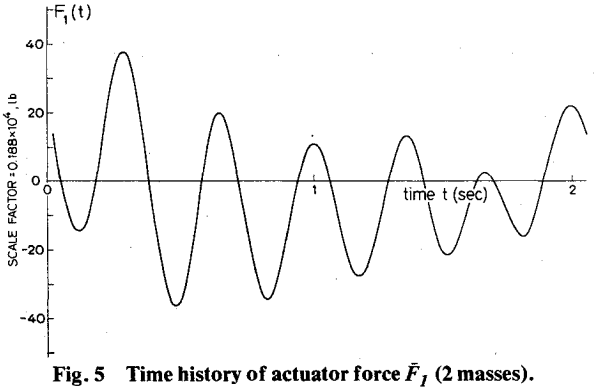

Fig. 5 Time history of actuator force $\bar{F}_1$ (2 masses).

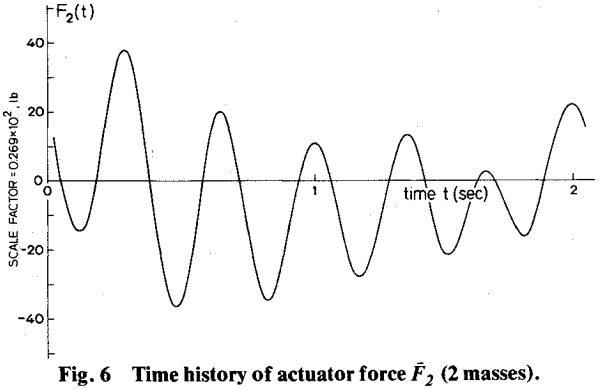

Fig. 6 Time history of actuator force $\bar{F}_2$ (2 masses).

in these graphs are only small portions of the total time history computed. The total length of the time history calculated was about 50 times to that shown in Figs. 5, 6, 10-12. In Example a), the computer time (on IBM 360/91) required to generate a set of two time histories of the total length just described is 20 sec. Similarly, the computer time for the set of five time histories in Example b) is 30 sec.

IV. Actuator Loading to Reproduce Combined Effect of Torsion and Bending

Consider a cross-section of a wing where the distributed load is acting through the aerodynamic center as shown in

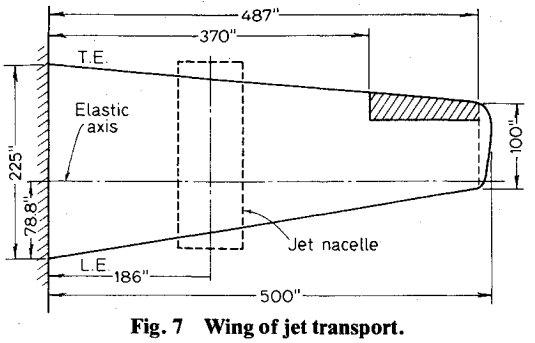

Fig. 7 Wing of jet transport.

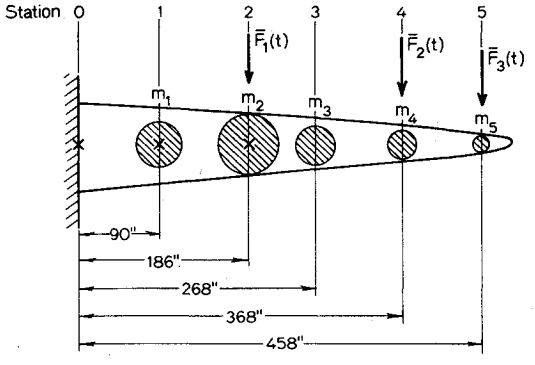

X : locations at which moments are computed

Fig. 8 Idealized jet transport wing (5 masses).

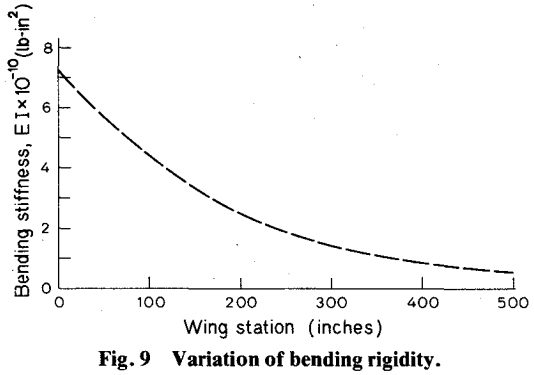

Fig. 9 Variation of bending rigidity.

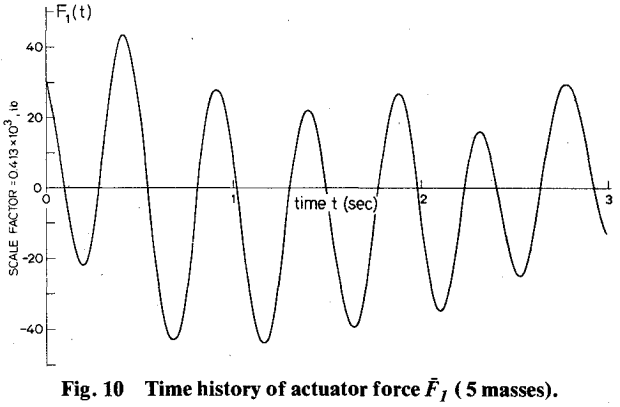

Fig. 10 Time history of actuator force $\bar{F}_1$ (5 masses).

Fig. 13. For the case with the straight elastic axis (x) along wing span, the lift loading $L(x,t)$, through the aerodynamic center can be transferred to an equivalent loading composed of lift and twisting moment which are acting through the elastic axis as shown in Fig. 14. The twisting moment can be expressed in terms of the lift by

$$T(x,t) = e(x)L(x,t) \tag{32}$$

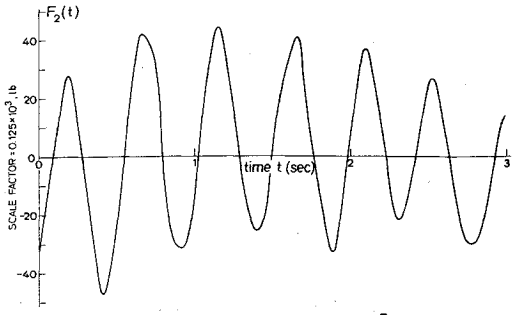

Fig. 11 Time history of actuator force $\bar{F}_2$ (5 masses).

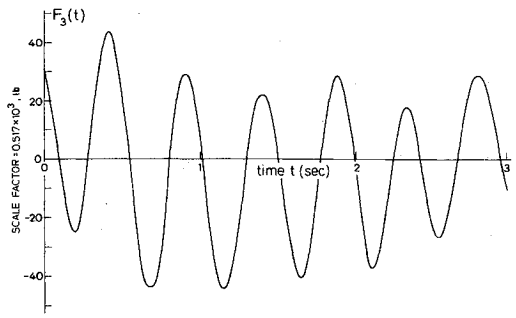

Fig. 12 Time history of actuator force $\bar{F}_3$ (5 masses).

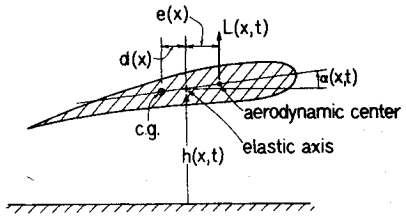

Fig. 13 Wing cross-section.

where $e(x)$ is the eccentricity of the elastic axis from the aerodynamic center. For a continuous system, the coupled equations of motion can be written as

$$\frac{\partial^2}{\partial x^2}\left(EI\frac{\partial^2 h}{\partial x^2}\right)+c_h\frac{\partial h}{\partial t}+m\frac{\partial^2 h}{\partial t^2}-md(x)\frac{\partial^2\alpha}{\partial t^2}=L(x,t) \tag{33}$$

$$\frac{\partial}{\partial x}\left(GJ\frac{\partial\alpha}{\partial x}\right)+c_\alpha\frac{\partial\alpha}{\partial t}-I_\alpha\frac{\partial^2\alpha}{\partial t^2}-md(x)\frac{\partial^2 h}{\partial t^2}=T(x,t)=e(x)L(x,t) \tag{34}$$

where h, α = vertical motion and torsional motion, respectively; c_h, c_α = damping coefficients of vertical and torsional motion, respectively; and m, I_α = mass and moment of inertia per unit span, respectively.

The analysis to obtain responses h and α can be extended to a discrete system in a similar manner as considered in previous sections for bending response without torsion. Following that procedure, the spectral density matrix $[S]$ associated with response bending and twisting moments, $M(x_\nu,t)$ and $T(x_\nu,t)$ evaluated at r stations $(x_0, x_1, x_2,\ldots,x_{r-1})$ of structural importance, will be obtained.

To determine the time histories of the actuator loading for laboratory testing, consider the actuator loads $\bar{F}_{1j}$, $\bar{F}_{2j}$ $(j=1,2,\ldots,r)$ to be applied at a set of r stations $(y_1, y_2,\ldots,y_r)$ as shown in Fig. 15. In this manner, both bending and twisting moments can be imposed to the wing when $\bar{F}_{1j}\neq\bar{F}_{2j}$.

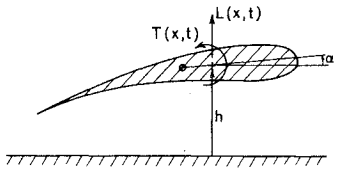

Fig. 14 Lift and moment loading on the wing.

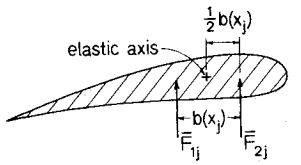

a)

Fig. 15 Actuator loading on a wing.

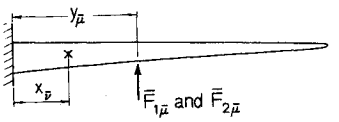

b)

The quasi-static bending and twisting moments $\bar{M}(x_{\bar\nu},t)$ and $\bar{T})x_{\bar\varphi}$ can then be written as

$$M(x_{\bar\nu},t)=\sum_{\bar\mu=\bar\nu+1}^{r}(y_{\bar\mu}-x_{\bar\nu})\{F_{1\bar\mu}(t)+F_{2\bar\mu}(t)\} \tag{35}$$

Inverting Eq. (35)

$$\bar{F}_{1j}+\bar{F}_{2j}=\sum_{\bar\nu=0}^{r-1}d_{j\bar\nu}\bar{M}(x_{\bar\nu},t) \tag{36}$$

where the elements $d_{j\bar\nu}$ are defined in Eq. (15).

The twisting moment d the elastic axis can be obtained from

$$\bar{T}(x_{\bar\nu},t)=\frac{1}{2}\sum_{\bar\mu=\bar\nu+1}^{r}b_{\bar\mu\bar\nu}[F_{1\bar\mu}(t)+F_{2\bar\mu}(t)] \tag{37}$$

where $b_{\bar\mu\bar\nu}$ is triangular matrix elements of torsional moment arm. Inverting the above,

$$\bar{F}_{1j}-\bar{F}_{2j}=2\sum_{\bar\nu=0}^{r-1}g_{j\bar\nu}\bar{T}(x_{\bar\nu},t) \tag{38}$$

where $j=1,2,\ldots,r$, and $g_{j\bar\nu}$ are inverse of $b_{j\bar\nu}$.

Solving Eqs. (36) and (38),

$$\bar{F}_{1j}=\sum_{\bar\nu=0}^{r-1}(d_{j\bar\nu}\bar{M}(x_{\bar\nu},t)+2g_{j\bar\nu}\bar{T}(x_{\bar\nu},t)) \tag{39}$$

$$\bar{F}_{2j}=\sum_{\nu=0}^{r-1}(d_{j\bar\nu}\bar{M}(x_{\bar\nu},t)-2g_{j\bar\nu}\bar{T}(x_{\bar\nu},t)) \tag{40}$$

After some manipulation, therefore, each component of the spectral density matrix $[S_{\bar F}]$ of $\bar{F}_{11}(t)$, $\bar{F}_{21}(t)$. $\bar{F}_{22}(t)$,..can be written in terms of the components of the spectral density matrix $[S]$ of $\bar{M}(x_1, t)$, $\bar{T}(x_1,t)$, $\bar{M}(x_2,t)$,... Usingthe equivalence $[\bar{S}]=[S]$, we can obtain the spectral density matrix $[S_{\bar F}]$ in terms of $[S]$. If $\bar{F}_{11}(t)$, $\bar{F}_{21}(t)$,..are generated on the basis of such matrix $[S_{\bar F}]$, these forces will produce the required bending and twisting moments (with inertia effect taken into consideration) at specified wing locations.

V. Conclusions

A method to generate time histories of actuator loading for large scale laboratory testing was presented. The computer

time necessary to perform these calculations was not expensive: it takes about 30 sec on IBM 360/91 to obtain one set of calculations which includes response spectral densities caused by gust and actuator loading, and time histories of actuator forces at five locations on the structure. The total time length of these histories computed was about 2 min.

The method of analysis considered in this study is fairly general but restricted to discrete elastic systems and stationary random inputs. However, a segmented nonstationary process, where gust loading is stationary within each segment but nonstationary from one segment to another, can be included in the formulation. Furthermore, the examples chosen are severe idealizations of an actual aircraft-gust interaction problem. The results shown correspond to the cases where gust loading is assumed to be spatially uniform over the wing surface, wing oscillations are restricted to vertical motions only, and nonsteady aerodynamic loads and rigid airplane modes are not included. If the structural motions and aerodynamic loading are within linear theory, the above can be included in the general formulation presented in a straightforward fashion.

Appendix: Simulation of Multivariate Random Processes

Consider a set of multivariate homogeneous Gaussian processes $\bar{F}_j(t)$ $(j=1,2,\ldots,r)$ with mean zero and cross spectral density matrix $[S]$ where $[S]$ is Hermitian and nonnegative definite. Then, it can be shown that a multivariate Gaussian process can be simulated by the following series (Ref. 7)

$$\bar{F}_j(t) = \sum_{n=1}^{j} \sum_{i=1}^{N} |R_{jn}(\omega_i)| (2\Delta\omega)^{1/2} \cdot \cos(\omega_i t + \theta_{jn}(\omega_i) + \psi_{ni}) \tag{A1}$$

In Eq. (A1), the lower triangular matrix $[R]$ is related to the cross-spectral density matrix $[S]$ by

$$[S] = [R][R^*]' \tag{A2}$$

and

$$\theta_{jn}(\omega_i) = \tan^{-1}\left\{ \frac{Im[R_{jn}(\omega_i)]}{Re[R_{jn}(\omega_i)]} \right\} \tag{A3}$$

with ψ_{ni} being realizations of independent random phase angles uniformly distributed between 0 and 2π, where * indicates complex conjugate and the prime transpose.

For larger N, the computation of multivariate random processes by Eq. (A1) can be time consuming since computation time is a function of N^2. To reduce computation time, Eq. (A1) is modified to accommodate the Fast Fourier Transform (FFT) technique. By applying a discrete inverse Fourier transform to a complex-valued quantity $Y(\omega_k)$, a discrete time history $y(t_n)$ can be obtained

$$y(t_n) = \sum_{k=1}^{N} Y(\omega_k) \exp i \frac{2\pi kn}{N} \tag{A4}$$

when $n=0, 1, 2\ldots, N-1$, and i = imaginary unit, $\omega_k = k/N\Delta t$, and $t_n = n\Delta t$, with Δt being the time increment.

Expressing Eq. (A1) in the form of Eq. (A4), we can show that

$$\bar{F}_j(t) = (2\Delta\omega)^{1/2} Re\{\bar{F}_j(t)\} \tag{A5}$$

in which $Re\{\bar{F}_j(t)\}$ represents the real part of $\bar{F}_j(t)$ and

$$\bar{F}_j(t) = \sum_{n=1}^{j} \sum_{k=1}^{N} |R_{jn}(\omega_k)| \cdot \exp i\{\theta_{jn}(\omega_k) + \psi_{nk}\} \exp i \frac{2\pi kn}{N} \tag{A6}$$

The advantage of Eq. (A6) is such that the multivariate random process can be computed using the FFT algorithm. Then, utilizing Eqs. (A5) and (A6), togehter with the specified cross-spectral density matrix, time histories of actuator forces $[\bar{F}(t)]$ can be obtained.

References

[1] Naumann, E.C., "Evaluation of the Influence of Load Randomization and of Ground-Air-Ground cycles on Fatigue Life," NASA TND-1954, Oct. 1964.

[2] Schijve, J., "The Analysis of Random Load-Time Histories with Relation to Ftigue Tests and Life Calculations," MP 201, Oct. 1960, Natl. Luchtwaartlab, Amsterdam.

[3] Schijve, J., Jacobs, F.A., and Tromp, P.H., "Crack Propagation in Aluminum Alloy Sheet Materials under Flight-Simulation Loading," NLR TR-68117u, National Lucht-Eu Ruimtevaartlaboratorium, Amsterdam.

[4] Schijve, J., Broek, D., and DeRijk, P., "Fatigue Tests with Random and Programmed Load Sequencies with and without Ground-to-Air Cycles: A Comparative Study on Full-Scale Wing Center Sections," NLR-TR S.613, Dec. 1965, National Lucht-Eu Ruimtevaartlaboratorium, Amsterdam.

[5] Swanson, S.R., "Random Load Fatigue Testing: A State of the Art Survey," presented at 70th Annual meeting, American Society for Testing and Materials, June 1967, Boston.

[6] Wilkins, D.J., Wolff, R.V., Cox, E.F., and Shinozuka, M., "Realism in Fatigue Testing: The Effect of Flight-by-Flight Thermal and Random Load Histories on Composite Bonded Joints," presented at ASTM Syjposium on Fatigue of Composite Materials, Dec. 1973, Bal Harbour, Fla.

[7] Shinozuka, M., and Jan. C.-M., "Digital Simulation of Random Processes and Its Applications," *Journal of Sound and Vibration*, Vol. 25, Feb. 1972, pp. 111-128.

[8] Shinozuka, M., "Digital Simulation of Random Processes in Engineering Mechanics with the Aid of FFT Technique," *Proceedings, Symposium on Stochastic Problems in Mechanics*, 1973, University of Waterloo.

[9] Liepman, H.W., "Extension of the Statistical Approach to Buffeting and Gust Response of Wings of Finite Span," *Journal of the Aeronautical Sciences*, Vol. 19, Dec. 1952, pp. 793-800.

[10] Howell, L.J., and Lin, Y.K., "Response of Flight Vehicles to Nonstationary Atmospheric Turbulence," *AIAA Journal*, Vol. 9, Nov. 1971, pp. 2,201-2,207.

[11] Houbolt, J.C., Steiner, R., and Pratt, K.G., "Dynamic Response of Airplanes at Atmospheric Turbulence Including Flight Data on Input and Response," TR-199, 1964.

[12] Bisplinghoff, R.L., Ashley, H., and Halfman, R.L., *Aeroelasticity*, Addison-Wesley Co., Inc., 1955.